Synthesis and Properties of Electrophosphorescent Chelating Polymers with Iridium Complexes in the Conjugated Backbone

Hongyu Zhen, Changyun Jiang, Wei Yang,* Jiaxing Jiang, Fei Huang, and Yong Cao*[a]

Abstract: The synthesis of electrophosphorescent chelating polymers by Suzuki polycondensation of A-A- and B-B-type monomers is described, in which the fluorene-*alt*-carbazole (PFCz) segment is used as polymer backbone. By using alkyl-substituted ligands of iridium complex monomers, chelating copolymers with higher contents of iridium complex can be synthesized. Chemical and photophysical characterization confirm that the Ir complex is incorporated into the polymer backbone as one of the monomer repeat units by means of two 5-bromotolylpyridine ligands. Chelating polymers with Ir complexes in the conjugated polymer backbone show highly efficient energy transfer of excitons from the PFCz host segment to the Ir complex by an intramolecular trapping mechanism. The external quantum and luminous efficiencies of a device made with PFCzMppyIrhm4 copolymer reach 4.1% ph/el (photons/electron) and 5.4 cd A^{-1}, respectively, at a current density of 32.2 mA cm^{-2}, an emission peak of 577 nm, and a luminance of 1730 cd cm^{-2}. Most important, the devices made from the chelating copolymers show no notable efficiency decay with increasing current density due to reduced concentration quenching and triplet–triplet (T–T) annihilation. This indicates that incorporation of the phosphorescent complex into the rigid conjugated polymer main chain is a new way to simultaneously realize high efficiency, long-term stability, and simple processing of phosphorescent polymer light-emitting diodes.

Keywords: chelates · iridium · luminescence · polymerization · polymers

Introduction

Recently, electrophosphorescent light-emitting diodes (LEDs), in which both singlet and triplet excitons contribute to light emission, have attracted great scientific and commercial attention because of their high quantum efficiency.[1] Iridium-based complexes are a popular choice as efficient dopants due to the relatively short phosphorescent lifetime[2] Green organic light-emitting diodes (OLEDs) with $[(ppy)_2Ir(acac)]$ (ppy = 2-phenylpyridine, acac = acetylacetonate) doped into 3-phenyl-4-(1′-naphthyl)-5-phenyl-1,2,4-triazole (TAZ) show a high external quantum efficiency of 19% ph/el and a power efficiency of 60 Lm W^{-1}.[3] The ease of fabrication by utilization of printing techniques and potential applications in large-area flat-panel displays at low power consumption make phosphorescent dye-doped polymer LEDs (PHPLEDs) extremely attractive.[4] Jiang et al.[5] reported red PLEDs in which $[(piq)_2Ir(acac)]$ (piq = 1-phenylisoquinolyl-N,$C^{2'}$) is doped into conjugated poly(9,9-dioctylfluorene) (PFO) and nonconjugated polyvinylcarbazole (PVK) with external quantum efficiencies of 12 and 10.2% ph/el, respectively, which demonstrate that conjugated and nonconjugated polymers can both be used as hosts with high external quantum efficiency.

Although devices in which phosphorescent dyes are doped into small-molecular or polymer hosts are successful in the realization of high-efficiency O/PLEDs, these dye-doped devices may undergo phase segregation, which leads to fast decay of efficiency with increasing current density. A solution to this problem is to introduce the phosphorescent dye into the polymer chain. Lee et al.[6] synthesized nonconjugated polyethylene main chains with phenylpyridine attached to side chains as a ligand and pendant *N*-vinylcarbazole as host material. High external quantum efficiency of 4.4% ph/el was achieved at a current density of 6.4 mA cm^{-2}. A similar approach of using a nonconjugated main chain with a pendant diketone was reported by Tokito et al.[7] High external quantum efficiencies of 5.5, 9, and

[a] H. Zhen, C. Jiang, Prof. W. Yang, J. Jiang, F. Huang, Prof. Y. Cao
Institute of Polymer Optoelectronic Materials and Devices
Key Laboratory of Specially Functional Materials and Advanced Manufacturing Technology
South China University of Technology, Guangzhou 510640 (China)
Fax: (+86)208-711-0606
E-mail: pswyang@scut.edu.cn
poycao@scut.edu.cn

 DOI: 10.1002/chem.200401090

3.5% in red, green, and blue PLEDs were respectively achieved. Phosphorescent conjugated polymers based on a polyfluorene backbone with diketone pendants attached to the C-9 position of fluorene were reported by Chen et al.[8] A device made from the graft polymer of 1.3 mol% [(btp)$_2$Ir(acac)] (btp = 2-(2′-benzo[4,5-α]thienyl)pyridinato-N,C$^{3'}$) with a diketone attached to the 9-position of the fluorene unit has an external quantum efficiency of 1.59% ph/el and a luminous efficiency of 2.8 cd A^{-1} at 7.0 V with a luminance of 65 cd m^{-2} and peak emission at 610 nm. A series of well-defined conjugated oligo- and polyfluorenyl bis-cyclometalated Ir complexes was synthesized by Suzuki homopolycondensation of A-B monomer by Sandee et al.[9] Maximum external quantum efficiencies of 1.5 and 0.12% ph/el were obtained, respectively, by introducing [(btp)$_2$Ir(acac)] and [(ppy)$_2$Ir(acac)] complexes covalently into a poly(9,9′-dioctylfluorene) backbone.

Recently, we reported that the intramolecular trapping may be a very quick and efficient process in a number of narrow-gap monomers incorporated into conjugated copolymers.[10] It would be interesting to investigate a chelating polymer with a phosphorescent metal complex as a repeat unit incorporated into a conjugated main chain. In this case, the conjugated segment plays two roles: polymer ligand and host for the energy-transfer system. High-efficiency energy transfer from the polymer host to the triplet metal complex in the polymer main chain by efficient intramolecular energy transfer would be expected. Besides Ir complexes, there are also many reports on the incorporation of other organometallic species into polymer main chains.[11] Wang et al.[12] synthesized two bipyridyl-phenylene-vinylene-based polymers for metal-ion sensor studies. Terpyridine-based metal coordination polymers were synthesized and characterized.[13] A series of poly(1,1′-ferrocenylene-4,4″-*p*-oligophenylenes) with high molecular weight was obtained by Pd-catalyzed polycondensation of haloaromatics and arylboronic acid derivatives.[14] Recently, a group of platinum-containing diyne and polyyne materials consisting of 9,9-dihexylfluorene, 9-butylcarbazole, and oligopyridine linkage units was prepared.[15]

Here we report the synthesis of chelating copolymers by Suzuki polycondensation of A-A- and B-B-type monomers by exploiting two bromine atoms in different ligands of iridium bis-chelate complexes. In such polycondensations, gelation of the reaction mixture or formation of highly insoluble products leads to incomplete metal chelation and to phosphor loadings lower than those targeted.[9] By using monomeric Ir complexes of alkyl-substituted ligands, that is, [(mppyBr)$_2$Ir(acac)] (mppyBr = 5-bromo-2-*p*-tolylpyridine-C$^{2'}$,N) and [(mppyBr)$_2$Ir(hmacac)] (hmacac = 2,2,6,6-tetramethyl-3,5-heptanedione), the solubility of Ir complexes is improved, gelation of the reaction mixture is avoided, and chelating copolymers with higher contents of Ir complex are synthesized. The fluorene-*alt*-carbazole segment was used as polymer backbone because the HOMO level of carbazole-based copolymers can be tuned by substitution at the 3-, 6-, and 9-positions, while the triplet level remains sufficiently high to accommodate even blue triplet emitters.[16]

Results and Discussion

Synthesis of the complexes and copolymers: The synthetic routes to the iridium bis-chelate complex monomers and the corresponding complexes with bromine-free ligands, which are the actual units in the copolymers, are depicted in Scheme 1. 5-Bromo-2-*p*-tolylpyridine was synthesized by a Pd-catalyzed cross-coupling reaction.[17] Since 2,5-dibromo-

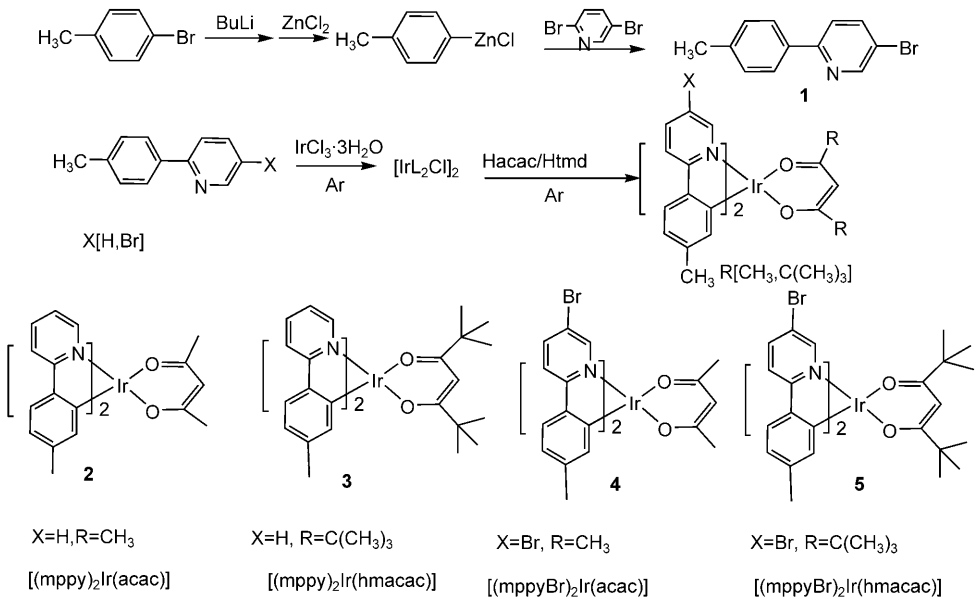

Scheme 1. Synthesis of the iridium complexes.

pyridine contains two reactive bromine atoms, we used arylzinc chloride, in which zinc has intermediate electronegativity, rather than highly electronegative lithium for the Pd-catalyzed cross-coupling reaction. As a result, the reaction takes place selectively at the 2-positon to give 5-bromo-2-tolylpyridines. In the reaction between the chloro-bridged dimmers and the β-diketonate, the yields of the iridium bis-chelate complex depend on the solubility of the products. Compared to the complexes with acac, those with hmacac are formed in higher yield. The synthetic routes to the corresponding chelating copolymers are depicted in Scheme 2. Brominated Ir complexes $[(mppyBr)_2Ir(acac)]$ and $[(mppyBr)_2Ir(hmacac)]$ copolymerized with dioxaborolanyldioctylfluorene in the presence of dibromocarbazole to form chelating copolymers by Suzuki polycondensation. The feed ratios of Ir complexes in the polycondensation were 1, 2, 4, 5, 10, and 20 mol%, and the corresponding copolymers are respectively named PFCzMppyIr1, PFCzMppyIr2, PFCzMppyIr5, PFCzMppyIr10 and PFCzMppyIrhm1, PFCzMppyIrhm4, PFCzMppyIrhm10, and PFCzMppyIrhm20.

The two brominated Ir complexes $[(mppyBr)_2Ir(acac)]$ and $[(mppyBr)_2Ir(hmacac)]$ differ in that the two Me groups of acac in the former are substituted by two *t*Bu groups in the latter. The resulting higher solubility in organic solvents leads to better compatibility with other comonomers and avoids gelation during copolymerization. The fact that copolymers PFCzMppyIrhm have a higher molecular weight and higher content of Ir complex in the chelating copolymers than PFCzMppyIr seems to support such a prediction (Table 1).

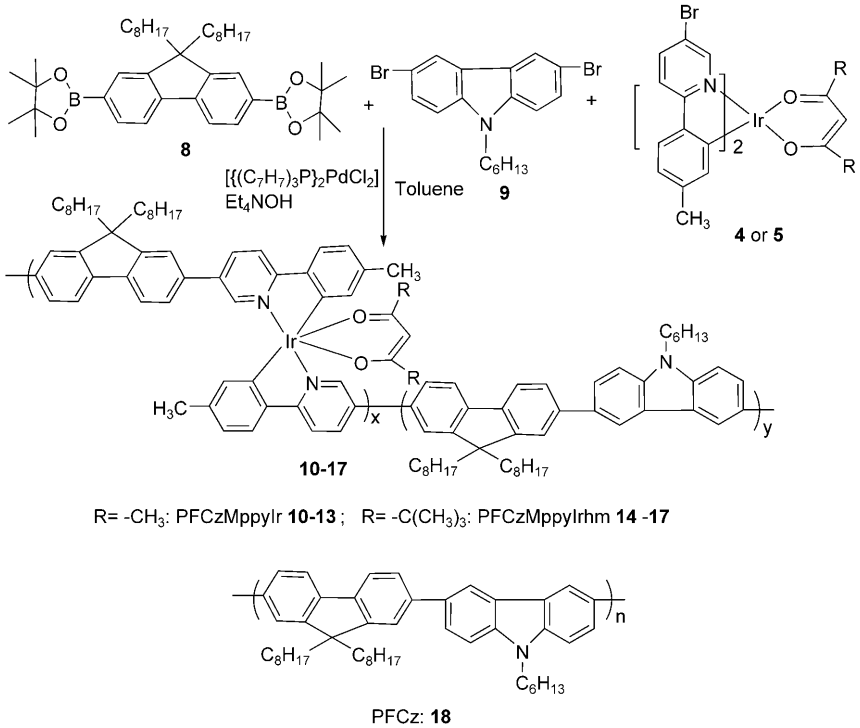

Scheme 2. Synthesis of the chelating copolymers.

Table 1. Molecular weights and composition of the copolymers.

Copolymer	$10^{-3} M_n$[a]	PDI	Complex content [mol%] in feed	in copolymer[b]
PFO	23.1	2.47	–	–
PFCz	6.5	1.58	–	–
PFCzMppyIr1	4.9	2.18	1	0.56
PFCzMppyIr2	6.6	1.45	2	0.65
PFCzMppyIr5	4.1	1.47	5	3.02
PFCzMppyIr10	4.3	1.52	10	4.79
PFCzMppyIrhm1	9.3	1.44	1	0.97
PFCzMppyIrhm4	17.0	1.42	4	3.41
PFCzMppyIrhm10	8.7	1.48	10	8.61
PFCzMppyIrhm20	8.2	1.50	20	15.89

[a] Number-average molecular weight M_n was estimated by GPC in THF by using a calibration curve of polystyrene standards. [b] Calculated from the carbon, nitrogen, and iridium content in the copolymers.

The iridium contents of copolymers were estimated by X-ray fluorescence (XRF) spectrometry. The molar ratio of Ir complex in the copolymers was calculated by combining XRF data with C, N elemental analyses (Table 1). The results indicate that Ir complexes were introduced into the polymer backbone, although the actual contents of Ir complex in the copolymers were slightly lower than that of the complex monomer in the feed. The ^{1}H NMR signal of the H atom between the two carbonyl groups in β-diketonate ligands with $\delta = 5.72$ is observable in the chelating copolymers with high contents of Ir complex (PFCzMppyIrhm20).

Optical and electrochemical properties: UV/Vis absorption spectra of $[(mppy)_2Ir(acac)]$ (mppyIr) and $[(mppy)_2Ir(hmacac)]$ (mppyIrhm) and photoluminescence (PL) spectrum of PFCz are shown in Figure 1. The good overlap between the emission spectra of the host (PFCz) and the absorption spectra of the guests (Ir complexes) meets the requirement for efficient Förster transfer from the host polymer to the Ir complexes in copolymers. The UV/Vis absorption spectra of the chelating copolymers PFCzMppyIr and PFCzMppyIrhm are shown in Figure 2a and b, respectively, along with the absorption spectra of PFCz copolymer. UV/Vis spectra of the chelating copolymers with low contents of Ir complex are dominated by a single peak with maximum absorbance around 350 nm, which is almost the same as that of the PFCz copolymer.[18] With increasing content of Ir complex, a weak absorption at 480 nm becomes observable

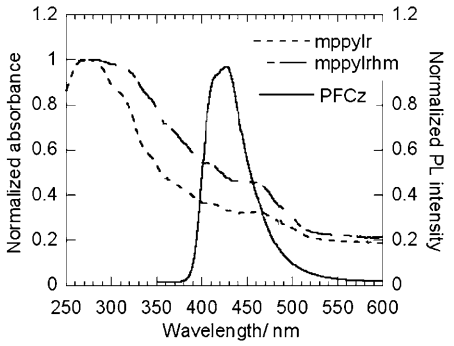

Figure 1. PL spectra of PFCz host polymer and UV/Vis absorption of the guest Ir complex in film.

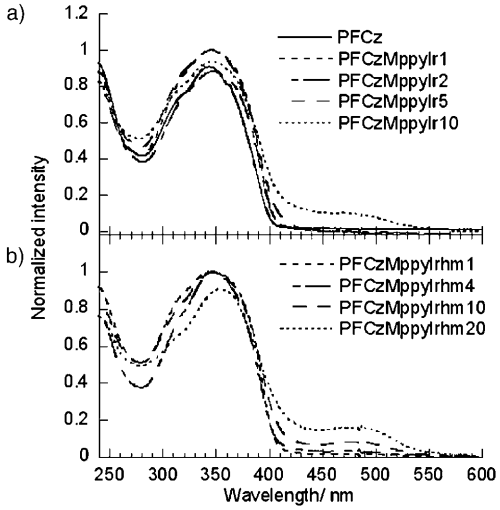

Figure 2. UV/Vis absorption spectra of the copolymers in film: a) PFCzMppyIr and b) PFCzMppyIrhm.

and the peak intensity increases, due to triplet metal-to-ligand charge-transfer (^{3}MLCT) transition.[19]

The redox behavior of the polymers was investigated by cyclic voltammetry (CV). All copolymers show a partial reversible oxidation wave with onset around 1.0–1.15 V; unfortunately, we failed to record the reduction peaks after many attempts. The HOMO levels of the copolymers were calculated according to the empirical formulas $E_{HOMO}/eV = -e(E_{ox}+4.4)$.[20] As shown in Table 2, the HOMO levels of homopolyfluorene (PFO) and PFCz are estimated as −5.76 and −5.52 eV, respectively. Thus, introduction of a carbazole unit into the PFO main chain raises the HOMO level. Similarly, there is a tendency for higher HOMO levels of copolymers with increasing content of Ir complex, which implies a lower barrier for hole injection in devices.[18] The optical band gaps E_{opt} were deduced from the absorption onset of the polymers. From the HOMO levels and the optical gaps, the LUMO levels of the polymers could be determined. The LUMO levels of carbazole-based copolymer are at about −2.4 eV (Table 2). This means a small barrier for election injection from the barium cathode used in this work, which has a work function of −2.2 eV.[21]

Table 2. Electrochemical properties of the copolymers in film.

Copolymer	E_{ox} [V]	HOMO [eV]	E_{opt}[a] [eV]	LUMO[b] [eV]
PFO	1.37	−5.77	2.76	−2.91
PFCz	1.12	−5.52	3.09	−2.43
CzMppyIr1	1.14	−5.54	3.07	−2.47
PFCzMppyIr2	1.16	−5.56	3.06	−2.50
PFCzMppyIr5	1.13	−5.53	3.03	−2.50
PFCzMppyIr10	1.10	−5.50	3.00	−2.50
PFCzMppyIrhm1	1.10	−5.50	3.05	−2.45
PFCzMppyIrhm4	1.10	−5.50	3.04	−2.46
PFCzMppyIrhm10	1.06	−5.46	2.98	−2.48
PFCzMppyIrhm20	0.98	−5.38	2.95	−2.43

[a] Estimated from the onset of the absorption edge attributed to the copolymer. [b] Calculated from the optical band gap E_{opt} and oxidation potential.

Photophysical properties: The PL spectra of the two kinds of chelating copolymers, compared with the corresponding blends of Ir complexes mppyIr and mppyIrhm doped into PFCz are shown in Figures 3 and 4. The contents of Ir complex in the blends are 1, 2, 3, and 8 mol% for mppyIr and 1, 2, 8, and 16 mol% for mppyIrhm. As can be seen from Figures 3a and 4a, the emission peak from the PFCz host segment at around 420 nm is almost completely quenched for both types of chelating copolymers. Only a weak emission at 420 nm can be observed for chelating copolymers even with 1 mol% of Ir complex, especially for PFCzMppyIrhm. The PL emission from Ir complexes is slightly red-shifted with increasing content of Ir complex from 575 nm for PFCzIrMppy1 to 585 nm for PFCzIrMppy10. In contrast, no significant red shift in PL emission can be observed for PFCzMppyIrhm (Table 3). For comparison, PL spectra of the pristine complexes mppyIr and mppyIrhm are shown in

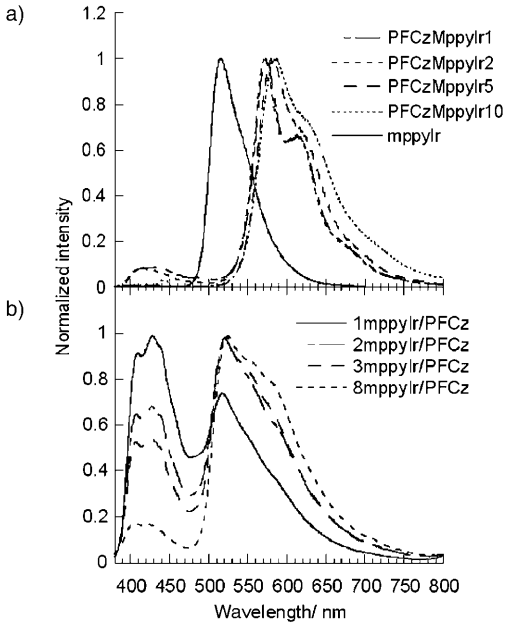

Figure 3. PL spectra in film of a) PFCzMppyIr copolymers and b) mppyIr/PFCz blends.

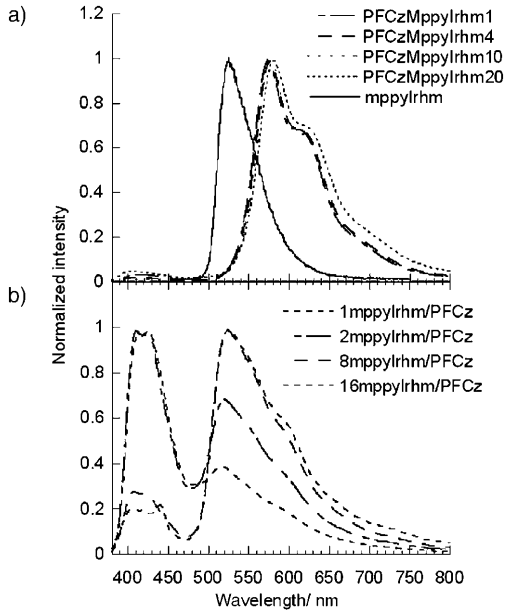

Figure 4. PL spectra in film of a) PFCzMppyIrhm copolymers and b) mppyIrhm/PFCz blends.

Table 3. Optical properties of the copolymers.

Copolymer	$\lambda_{abs.max}$ [nm]	Photoluminescence	
		λ_{PL} [nm]	Q_{PL} [%]
PFO	385	435	51
PFCz	350	410	42
PFCzMppyIr1	350	410, 575	25
PFCzMppyIr2	350	410, 575	35
PFCzMppyIr5	350	585	34
PFCzMppyIr10	350, 480	585	12
PFCzMppyIrhm1	350	410, 575	31
PFCzMppyIrhm4	350	575	21
PFCzMppyIrhm10	350, 485	575	17
PFCzMppyIrhm20	350, 485	580	6

Figures 3a and 4a, respectively. The PL spectra of both chelating copolymers are red-shifted by around 50–60 nm compared with the PL emission of pristine complexes mppyIr and mppyIrhm. To determine the origin of this significant red shift in PL emission of chelating copolymers relative to pristine small-molecule complexes, a study was made of the PL spectra of the blends from corresponding small molecular complexes doped into PFCz copolymers (Figures 3b and 4b). The PL emissions from Ir complexes in the doped systems are almost identical with those of the pristine small-molecule complexes (Figures 3a and 4a). Therefore, the significant red shift in PL emission for chelating copolymers must be related to the incorporation of Ir complexes into the polymer main chain. Judged from the structure of the chelating copolymer (Scheme 2), it is reasonable to conclude that the red shift in PL emission is due to the extended conjugation length of tolylpyridine, which is in conjugation with a neighboring fluorene segment in the chelating copolymers. The significant red shift of the emission peak in the chelating copolymers in comparison with that of guest–host blended system provides strong evidence that Ir complexes are indeed incorporated into the polymer main chain. The fact that extending the conjugation length in ligand of phosphorescent complexes will generally shift PL emission to lower energy was reported previously.[9,16a,22]

Comparing PL spectra of chelating polymers in Figures 3a and 4a with those of blend films (Figures 3b and 4b), it is noteworthy that the PL spectrum of PFCzMppyIr1 (actual content of Ir complex in the polymer is 0.56 mol%) resembles the PL spectra of 8mppyIr/PFCz (doping concentration of 8%) in terms of the quenching of PFCz emission (Figure 3b). It was reported that complete quenching of host PL emission in guest–host blended systems required 4–8% loading of phosphorescent complexes.[23] A significantly lower complex loading is required for complete quenching of host emission in the chelating conjugated copolymer in this study, and this suggests that intramolecular energy transfer is much more efficient than intermolecular energy transfer between guest–host systems. Further evidence for the relative roles of intra- and interchain interaction in energy transfer from host to guest can be obtained from the PL spectra in solution. Figure 5 compares PL spectra of the chelating copolymer PFCzMppyIrhm20 (Figure 5a) with that of 20 mppyIrhm/PFCz blend (Figure 5b) in THF solution. The chelating copolymer clearly shows much more efficient energy transfer than the Ir complex/PFCz blend. For chelating copolymer PFCzMppyIrhm20, emission of the PFCz segment was quenched completely at a solution concentration of around 0.1 M, while a strong PFCz emission remained at concentration of 1 M for the 20mppyIrhm/PFCz blend. Since both the molar ratios of Ir complex to PFCz or PFCz segment of copolymers in solution are almost equal, the difference in PL spectra must originate from the different structures of the two systems. In the blended system,

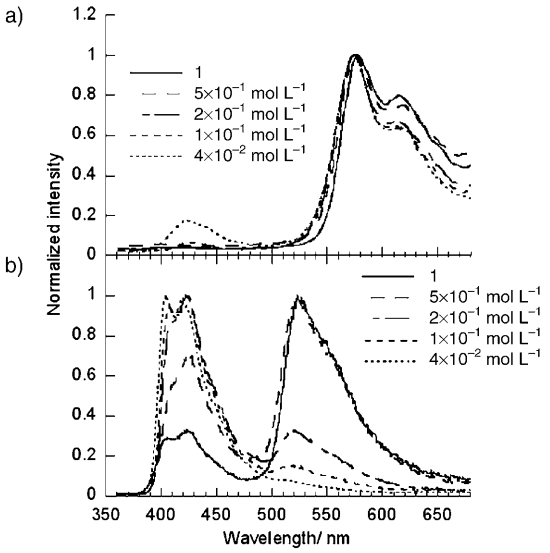

Figure 5. PL spectra in THF solution of different concentration of a) PFCzMppyIrhm20 copolymer and b) 20mppyIrhm/PFCz blend.

energy transfer is exclusively intermolecular, while for the chelating copolymer both intra- and interchain interactions contribute to energy transfer. Significantly more efficient energy transfer of the chelating copolymers unambiguously indicates that intramolecular energy transfer in these systems is a more efficient process. The PL efficiencies of copolymer films were measured in an integrating sphere under 325 nm excitation of an HeCd laser. Introducing Ir complex into the polymer main chain reduces PL efficiency (Table 3). The PL efficiencies decrease with increasing content of Ir complex in the copolymers.

Electroluminescent properties: Figures 6a and 7a show the electroluminescnce (EL) spectra of devices made from chelating copolymers. Compared with PL spectra (Figure 3, Figure 4), PFCz host emission at 420 nm in EL spectra is

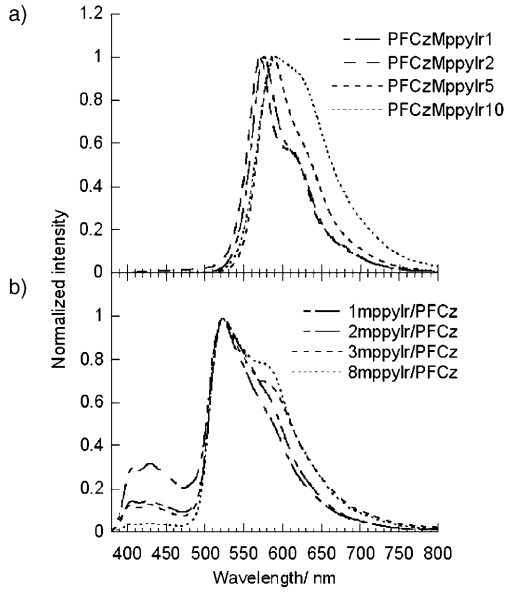

Figure 6. EL spectra of a) PFCzMppyIr copolymers and b) mppyIr/PFCz blends. Device structure: ITO/PEDOT/copolymer (or blend)+PBD (30 wt%)/Ba/Al.

completely quenched for devices made from all copolymers with contents of Ir complex as low as 1%. Complete quenching of host EL emission at lower concentration of Ir complex than that of PL emission was reported by many authors,[23b,24] and is evidence that the dominant emission mechanism in such systems is charge trapping (rather than Förster energy transfer) followed by recombination on an Ir-complex unit. A slight red shift of EL emission is observed from 570 nm for PFCzMppyIr1 to 590 nm for PFCzMppyIr10 (Figure 6a). Like in the case of PL emission, no obvious red shift can be observed for PFCzMppyIrhm. In comparison, the EL spectra of the devices made from corresponding blends of mppyIr and mppyIrhm doped into PFCz copolymer are shown in Figures 6b and 7b, respectively. Like the case of PL emission, EL peaks for chelating copolymers are also red-shifted by 50–60 nm in comparison

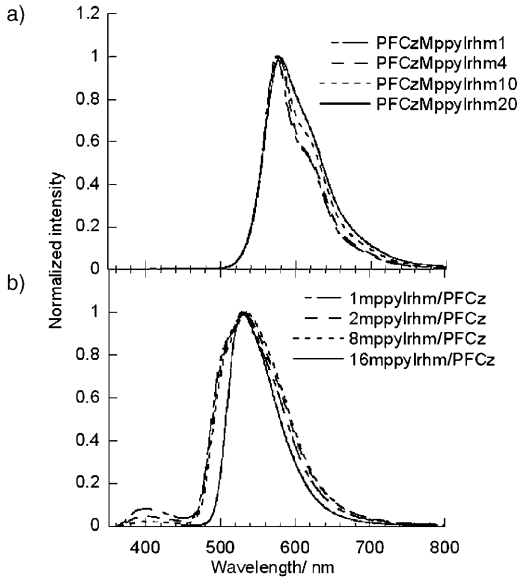

Figure 7. EL spectra of a) PFCzMppyIrhm copolymers and b) mppyIrhm/PFCz blends. Device structure: ITO/PEDOT/PVK/polymer (or blend)/Ba/Al.

with the blended systems. As discussed in the case of PL emission, this is the result of the extended conjugation length of ligands due to the incorporation of tolylpyridine into the polymer main chain. Comparing EL spectra of the devices made from chelating copolymers (Figures 6a and 7a) with those of the devices made from blends (Figures 6b and 7b) reveals that the former show much more efficient energy transfer than the latter, which again indicates that intramolecular trapping along the conjugated polymer chain is a more efficient energy-transfer process. We also note that the devices made from mppyIrhm/PFCz blends show much more quenching of host emission at low content of complex (Figure 7b) than those from the blends of mppyIr/PFCz (Figure 6b), which indicates much more efficient energy transfer in the former. Since the difference between the two complexes is only in more bulky substitution (*t*Bu instead of Me) of the β-diketonate in the former, the more efficient energy transfer is obviously due to better compatibility between guest and PFCz host in mppyIrhm/PFCz blends.[23b] Most important, in contrast to the significant influence in compatibility in phosphorescent dye/host blended systems, both chelating copolymers show much less difference in energy-transfer efficiencies (Figures 6a and 7a). This again indicates that intrachain (via conjugated main chain) energy transfer is more efficient in the chelating copolymers than interchain interaction. Since the dominant energy-transfer mechanism in chelating copolymers is intramolecular, it is less sensitive to polymer morphology. This indicates another advantage of incorporating phosphorescent dye into conjugated polymer main chain over blended systems.

Preliminary device performance (although not optimized) is encouraging (Table 4). Copolymers with different contents of Ir complex were used as the emitting layer in a light-emit-

Table 4. Device performance of the copolymers.

Copolymer	λ_{max} [nm]	Bias [V]	J [mA cm^{-2}]	Luminance [cd m^{-2}]	Efficiency QE$_{ext}$ [%]	LE [cd A^{-1}]
PFCzMppyIr1[a]	570	11.5	39	1160	1.3	3.0
PFCzMppyIr2[a]	570	7.2	39.8	680	0.9	1.7
PFCzMppyIr5[a]	585	12.0	34.7	660	1.2	1.9
PFCzMppyIr10[a]	590	18.7	34.2	470	1.3	1.4
PFCzMppyIrhm1[b]	575	12.5	33.5	1150	2.8	3.4
PFCzMppyIrhm4[b]	575	13.0	32.2	1730	4.1	5.4
PFCzMppyIrhm10[b]	577	15.7	33.3	780	1.8	2.4
PFCzMppyIrhm20[b]	577	17.0	36.4	580	1.4	1.6

[a] ITO/PEDOT/copolymer + PBD (30 wt %)/Ba/Al. [b] ITO/PEDOT/PVK/copolymer/Ba/Al.

ting device with the configuration ITO/PEDOT/PFCzMppyIr + 30% PBD/Ba/Al and ITO/PEDOT/PVK/PFCzMppyIrhm/Ba/Al. PBD was blended into PFCzMppyIr copolymers to increase the electron-transport capability, in accordance with several previous reports.[5,18a] Device performance from PFCzMppyIr + 30% PBD blends are listed in Table 4. We note that the device efficiencies from PFCzMppyIr without PBD are around 30% lower than those with PBD (data for device without PBD are not listed in Table 4). The external quantum efficiencies of the devices made from PFCzMppyIr containing 30% of PBD reach 1.2–1.3% at a current density of around 35 mA cm^{-2} with no significant variation with copolymer composition (Table 4). Device efficiencies for copolymers PFCzMppyIrhm are much higher than those for PFCzMppyIr, especially for devices without PBD. The best device performance was achieved by PFCzMppyIrhm4 at a current density of 32.2 mA cm^{-2}, for which the external quantum and luminous efficiencies respectively reached 4.1% and 5.4 cd A^{-1}, with a luminance of 1730 cd m^{-2}. At a current density of 5.7 mA cm^{-2}, a maximum external quantum efficiency of 4.7% and a luminous efficiency of 6.1 cd A^{-1} are obtained, among the highest reported for polymer phosphorescent emitters. Figure 8 compares the current density J and luminance L versus bias voltage for the devices made from the copolymer PFCzMppyIrhm4 and the blend 4mppyIrhm/PFCz with the same concentration of Ir complex (4%). The device made from chelating copolymer shows a sharper exponential rise in J–V after turning on, a lower operating voltage, and higher efficiency. Other chelating copolymers show a similar tendency. This clearly indicates a much better device performance from chelating polymers compared to blended systems. Figure 9 shows the external quantum efficiency as a function of current density for devices made from two chelating copolymers. Unlike the phosphorescent devices made from dye-doped blends (either small-molecule or polymer host), which show a sharp decay in device efficiency with increasing current density,[18] the device efficiencies of the chelating

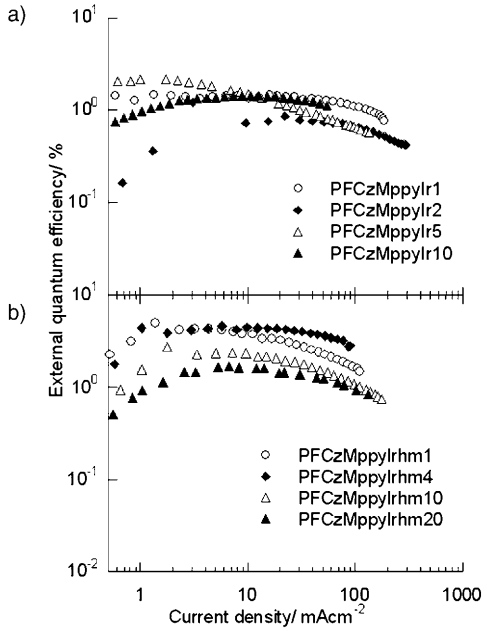

Figure 9. External quantum efficiency versus current density of the devices made from copolymers: a) PFCzMppyIr; device structure: ITO/PEDOT/PFCzMppyIr + PBD (30 wt %)/Ba/Al. b) PFCzMppyIrhm; device structure: ITO/PEDOT/PVK/PFCzMppyIrhm/Ba/Al.

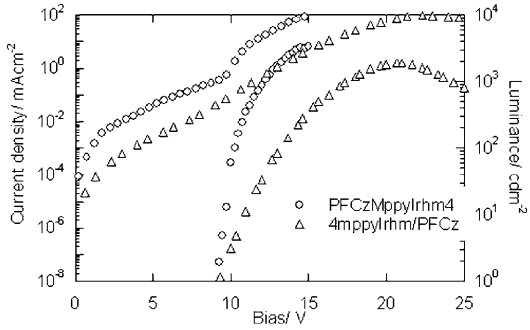

Figure 8. Comparison of J–V and L–V curves of the devices made from PFCzMppyIrhm4 copolymer and 4mppyIrhm/PFCz blend. Device structure: ITO/PEDOT/PVK/polymer (or blend)/Ba/Al.

polymers in this study initially increase slightly with increasing current density, and show essentially no decay with further increase in current density up to 100 mA cm^{-2}.This indicates that incorporation of phosphorescent complexes into the polymer main chain may have an advantage in suppressing concentration quenching and T–T annihilation, which are the primary quenching mechanisms for blended systems at high current density.[25] We also note that the decay pattern essentially does not change with increasing content of complex in the copolymer up to 20 mol % Ir complex in the copolymer (PFCzMppyIrhm20, Figure 9). This indicates that the incorporation of phosphorescent complexes into the

rigid conjugated polymer main chain prohibits aggregation of phosphorescent complexes and thereby reduces concentration quenching.[26]

Conclusion

In summary, we have demonstrated the efficient synthesis of chelating copolymers with Ir complexes incorporated into a conjugated polymer backbone by Suzuki polycondensation involving brominated tolylpyridine in the 5-position of a pyridine unit. Photophosphorescence and electrophosphorescence studies reveal that such chelating polymers with Ir complexes in the main chain show highly efficient energy transfer of excitons from the host segment (PFCz) to the Ir complexes by an intramolecular trapping mechanism. The more efficient energy transfer observed in chelating copolymers versus the corresponding blended systems of the same composition unambiguously indicates that intramolecular energy transfer is a more efficient process than interchain interaction. The best device performance in two series of chelating copolymers was realized with copolymer PFCzMppyIrhm4. External quantum efficiency of 4.1% and luminous efficiency of 5.4 $cd\,A^{-1}$ with a luminance of 1730 $cd\,cm^{-2}$ and an emission peak of 577 nm at a current density of 32.2 $mA\,cm^{-2}$ were realized. Most important, devices made from chelating copolymers are free of the efficiency decay with increasing current density and increasing content of Ir complex which is common to phosphorescent dye/host blended systems.

Experimental Section

Measurements: ^1H and ^{13}C NMR spectra were recorded on a Bruker DRX 400 spectrometer operating respectively at 400 and 100 MHz in $CDCl_3$ with TMS as reference. The molecular weight of the polymers was determined by Waters GPC 2410 in THF. Number-average (M_n) and weight-average (M_w) molecular weights were estimated by using a calibration curve of polystyrene standards. Elemental analyses were performed on Vario EL Elemental Analysis Instrument (Elementar Co.). Iridium content was determined by using a Philips (Magix PRO) sequential X-ray fluorescence (XRF) spectrometer with a rhodium tube operated at 60 kV and 50 mA, a LiF 200 crystal, and a scintillation counter. [Ir^{III}-(acac)$_3$] (Alfa Aesar Co.) was used as standard. Samples were prepared as homogeneous tablets (∅ 30 mm) of compressed (375 MPa) powder of the copolymers. UV/Vis absorption spectra were recorded on a HP 8453 spectrophotometer. The PL quantum yields were determined in an Integrating Sphere IS080 (LabSphere) with 325 nm excitation of a HeCd laser (Melles Griot). PL spectra of the copolymer solution were obtained on a Fluorolog-3 Spectrometer (Jobin-Yvon) with 90° angle detection. PL spectra of the copolymers in thin films on a quartz substrate were recorded on an Instaspec IV CCD spectrophotometer (Oriel Co.) under 325 nm excitation of an HeCd laser. Cyclic voltammetry was carried out on a Potentiostat Galvanostat Model 283 (Princeton Applied Research) with platinum working electrodes at a scan rate of 50 $mV\,s^{-1}$ against a calomel reference electrode with a nitrogen-saturated acetonitrile (CH_3CN) solution of 0.1 M tetrabutylammonium hexafluorophosphate (Bu_4NPF_6).

Materials: All manipulations involving air-sensitive reagents were performed in an atmosphere of dry argon. The solvents (THF, toluene) were purified by routine procedures and distilled under dry argon before use. All reagents, unless otherwise specified, were obtained from Aldrich, Acros, and TCI Chemical Co. and were used as received.

5-Bromo-2-*p*-tolyl-pyridine (1) was synthesized by the method reported by Jefferson and Sonja.[17] 1-Bromo-4-methylbenzene (8.14 g, 47.6 mmol) was added dropwise to a solution of of *n*-butylithium in hexane (1.6 M, 31.3 mL, 50 mmol) in THF (50 mL). When addition was complete, the reaction mixture was allowed to stir at −70 °C for 40 min. Zinc chloride (6.48 g, 47.6 mmol) was introduced into the solution through double-tipped syringe needle under argon pressure. After the resulting mixture had warmed to room temperature over 30 min, [$Pd(PPh_3)_4$] (0.6 g, 0.85 mmol) suspended in THF (50 mL) was added. After stirring at room temperature for 15 min, 2,5-dibrompyridine (11.0 g, 46.6 mmol) was added to the reaction mixture, and the resulting mixture was stirred at room temperature for 18 h. The reaction mixture was concentrated by evaporation of solvents, and the residue was dissolved in ethyl acetate, washed with water and a saturated aqueous solution of sodium chloride, and dried over anhydrous sodium carbonate. After evaporation of the solvent, the obtained product was purified by column chromatography (silica gel, 2% ethyl acetate/hexane) (yield 70%). ^1H NMR (400 MHz, $CDCl_3$): $\delta = 8.71$ (s, 1H), 8.02 (d, 1H), 7.78 (d, 1H), 7.76 (d, 2H), 7.20 (d, 2H), 1.54 ppm (s, 3H); elemental analysis (%) calcd for $C_{12}H_{10}BrN$: C 58.06, H 4.03, N 5.65; found: C 57.98, H 4.08, N 5.60.

[(mppy)$_2$Ir(acac)] (2) was prepared according to the published procedure.[27] Iridium trichloride hydrate (178 mg, 0.56 mmol), 2-*p*-tolylpyridine (282 mg, 1.68 mmol), 2-ethoxyethanol (10 mL), and water (5 mL) were added to a three-neck flask (100 mL). The mixture was refluxed under an Ar atmosphere for 24 h and then cooled to room temperature. The yellow precipitate was collected by filtration and washed with water and ethanol several times. The resulting yellow solid was purified by recrystallization from CH_2Cl_2/hexane. Then the dried product (476 mg, 0.078 mmol) was mixed with acetylacetone (22 mg, 0.22 mmol) and sodium carbonate (13 mg) in degassed 2-ethoxyethanol (8 mL) in a three-neck flask. The mixture was refluxed in an argon atmosphere for 13 h. After the mixture had been cooled to room temperature, a yellow-orange precipitate formed, which was collected by filtration, washed with water and methanol, and purified by column chromatography (silica gel, dichloromethane) to give a yellow powder (yield 75%). ^1H NMR (400 MHz, $CDCl_3$): $\delta = 8.47$ (d, 2H), 7.76 (d, 2H), 7.67 (t, 2H), 7.42 (d, 2H), 7.07 (t, 2H), 6.62 (d, 2H), 6.06 (s, 2H), 5.18 (s, 1H), 2.04 (s, 6H), 1.76 ppm (s, 6H); elemental analysis (%) calcd for $C_{29}H_{27}IrN_2O_2$: C 55.50, H 4.30, N 4.47; found: C 55.32, H 4.48, N 4.21.

[(mppy)$_2$Ir(hmacac)] (3) was prepared by following a similar procedure as for [(mppy)$_2$Ir(acac)] except that the acetylacetone was replaced by 2,2,6,6-tetramethyl-3,5-heptanedione (yield 85%). ^1H NMR (400 MHz, $CDCl_3$): $\delta = 8.34$ (d, 2H), 7.75 (d, 2H), 7.65 (t, 2H), 7.42 (d, 2H), 7.10 (t, 2H), 6.60 (d, 2H), 6.16 (s, 2H), 5.44 (s, 1H), 2.06 (s, 6H), 0.87 ppm (s, 18H); elemental analysis (%) calcd for $C_{35}H_{39}IrN_2O_2$: C 59.07, H 5.49, N 3.94; found: C 58.93, H 5.58, N 3.80.

[(mppyBr)$_2$Ir(acac)] (4) was prepared by following a similar procedure as for [(mppy)$_2$Ir(acac)] **(2)** except that 2-*p*-tolylpyridine was replaced by 5-bromo-2-*p*-tolylpyridine (yield, 70%). ^1H NMR (400 MHz, $CDCl_3$): $\delta =$ 8.50 (s, 2H), 7.81 (d, 2H), 7.69 (d, 2H), 7.46 (d, 2H), 6.60 (d, 2H), 6.02 (s, 2H), 5.23 (s, 1H), 2.10 (s, 6H), 1.80 ppm (s, 6H); elemental analysis (%) calcd for $C_{29}H_{25}Br_2IrN_2O_2$: C 44.27, H 3.18, N 3.56; found: C 44.15, H 3.36, N 3.48.

[(mppyBr)$_2$Ir(hmacac)] (5) was prepared by following a similar procedure as described above except that the acetylacetone was replaced by 2,2,6,6-tetramethyl- 3,5-heptanedione (yield 80%). ^1H NMR (400 MHz): $\delta = 8.42$ (s, 2H), 7.74 (d, 2H), 7.64 (d, 2H), 7.39 (d, 2H), 6.62 (d, 2H), 6.13 (s, 2H), 5.52 (s, 1H), 2.08 (s, 6H), 0.93 ppm (s, 18H); elemental analysis (%) calcd for $C_{35}H_{37}Br_2IrN_2O_2$: C 48.22, H 4.25, N3.21; found: C 48.03, H 4.42, N 3.00.

2,7-Dibromofluorene (6) and 2,7-dibromo-9,9-dioctylfluorene (7) were prepared according to the published procedures.[28]

2,7-Bis(4,4,5,5-tetramethyl-1,3,2-dioxaborolan-2-yl)-9,9-dioctylfluorene (8) was prepared following the published procedure from 2,7-dibromo-9,9-dioctylfluorene (**7**).[29] The resulting boronic ester was recrystallized

from methanol and further purified by column chromatography (silica gel, 10% ethyl acetate in hexane) to give a white solid (yield 50%). m.p. 128–131 °C. ^{1}H NMR (400 MHz, $CDCl_3$): $\delta = 7.81$ (d, 2H), 7.76 (s, 2H), 7.72 (d, 2H), 1.97 (m, 4H), 1.37 (s, 24H, CH_3), 1.22–0.98 (m, 20H), 0.81 (t, 6H), 0.54 ppm (m, 4H); elemental analysis (%) calcd for $C_{41}H_{64}O_4B_2$: C 76.74, H 10.04; found: C 76.43, H 9.95.

3,6-dibromo-9-*n*-hexylcarbazole (9) was prepared according to the published procedure.[30] ^{1}H NMR (400 MHz, $CDCl_3$): $\delta = 8.09$ (s, 2H), 7.53 (d, 2H), 7.24 (d, 2H), 4.17 (t, 2H,), 1.81–1.24 (m, 8H), 0.85 ppm (t, 3H); elemental analysis (%) calcd for $C_{18}H_{19}Br_2N$: C 52.81, H 4.64, N 3.42; found: C 52.72, H 4.83, N 3.22.

General procedure for Suzuki polycondensation taking PFCzMppyIr1(10) as an example:[31] **8** (341 mg, 0.5 mmol), **9** (200 mg, 0.49 mmol), [(mppyBr)$_2$Ir(acac)] (8 mg, 0.01 mmol), and bis(tri-o-tolyphosphine)palladium dichloride (5 mg) were dissolved in toluene/THF (1/1, 15 mL), stirred for 0.5 h, and then an aqueous solution of Et_4NOH (20%, 4 mL) was added. The mixture was heated to 100 °C and stirred for 2 d under argon. Then the polymer was capped by adding 2-(4,4,5,5-tetramethyl-1,3,2-dioxaborolan-2-yl)-9,9-dioctylfluorene (50 mg) with continued stirring for 12 h, and then bromobenzene (0.25 mL), followed by continued reaction for a further 12 h. The whole mixture was poured into methanol. The precipitated polymer was recovered by filtration and purified by chromatography on silica column with toluene to remove molecular complex and catalyst residue (yield, 50%). ^{1}H NMR (400 MHz, $CDCl_3$): $\delta = 8.50$ (2H), 7.51–7.84 (11H), 4.39 (2H), 2.04–2.14 (4H), 1.95 (2H), 1.11–1.52 (7H), 1.1 (24H), 0.74–0.89 ppm (16H); ^{13}C NMR (100 MHz, $CDCl_3$): $\delta = 151.70$, 141.04, 140.85, 140.41, 139.60, 133.10, 126.16, 125.53, 123.64, 121.68, 119.88, 118.96, 109.04, 78.10, 77.31, 76.99, 76.68, 55.36, 40.64, 31.80, 31.64, 30.11, 29.24, 29.07, 27.03, 23.91, 22.58, 14.02 ppm; elemental analysis (%) calcd: C 87.86, H 9.24, N 2.21; found: C 88.2, H 9.22, N 1.67.

PFCzMppyIr2 (11): Prepared from **8** (0.5 mol), **9** (0.48 mol) and [(mppyBr)$_2$Ir(acac)] (0.02 mol). Yield: 49%. ^{1}H NMR (400 MHz, $CDCl_3$): $\delta = 8.50$ (2H), 7.51–7.84 (11H), 4.39 (2H), 2.04–2.14 (4H), 1.95 (2H), 1.25–1.53 (7H), 1.1 (24H), 0.74–0.90 ppm (16H); ^{13}C NMR (100 MHz, $CDCl_3$) $\delta = 151.70$, 140.84, 140.40, 139.56, 133.10, 126.14, 125.52, 123.63, 121.67, 119.87, 118.95, 109.03, 77.30, 76.99, 76.67, 55.35, 43.41, 40.63, 31.79, 31.63, 30.10, 29.23, 29.06, 27.02, 23.90, 22.57, 14.01 ppm; elemental analysis (%) calcd: C 87.24, H 9.15, N 2.23; found: C 88.13, H 9.90, N 1.70.

PFCzMppyIr5 (12): Monomer feed: **8** (0.5 mol), **9** (0.45 mol), and [(mppyBr)$_2$Ir(acac)] (0.05 mol). Yield: 46%. ^{1}H NMR (400 MHz, $CDCl_3$): $\delta = 8.52$ (2H), 7.85–7.87 (10H), 7.75 (3H), 7.67, 7.55 (2H), 7.27 (2H), 4.2 (2H), 2.10 (6H), 2.08, 1.81, 1.56 (2H), 1.37 (6H), 1.28 (2H), 1.10–1.14 (20H), 0.90–0.92 (5H), 0.79–0.86 ppm (4H); ^{13}C NMR (100 MHz, $CDCl_3$): $\delta = 165.62$, 163.97, 151.70, 140.84, 140.41, 139.56,133.10, 126.73, 126.14, 125.54, 123.63, 121.63, 119.89, 118.95, 109.04, 77.31, 76.99, 76.68, 55.35, 55.17, 43.41, 40.63,31.79, 31.63, 30.09, 29.70, 29.23, 29.06, 27.02, 23.90, 23.61, 22.58, 14.02 ppm; elemental analysis (%) calcd: C 85.48, H 8.92, N 2.28; found: C 83.76, H 9.10, N 1.78.

PFCzMppyIr10 (13): Monomer feed: **8** (0.5 mol), **9** (0.4 mol), and [(mppyBr)$_2$Ir(acac)] (0.1 mol) Yield: 47%. ^{1}H NMR (400 MHz, $CDCl_3$): $\delta = 8.51$ (2H), 7.85–7.69 (11H), 7.6 (5H), 7.67, 7.55, 6.6, 6.25, 4.32 (2H), 2.24–1.97 (12H), 1.47–1.26 (9H), 1.12 (36H), 0.90–0.76 ppm (22H); ^{13}C NMR (100 MHz, $CDCl_3$): $\delta = 151.72$, 141.07, 140.88, 140.44,139.59, 138.14, 128.77, 127.21, 126.19, 125.56, 123.67, 121.70, 119.90, 118.98, 109.07, 77.34, 77.02, 76.70, 55.38, 55.20, 43.44, 40.65, 40.52, 31.81, 31.65, 30.12, 29.25, 29.09, 27.04, 23.93, 22.60, 14.03 ppm; elemental analysis (%) calcd: C 82.87, H 8.45, N 2.36; found: C 81.60, H 8.87, N 2.63.

PFCzMppyIrhm1 (14): Monomer feed: **8** (0.5 mol), **9** (0.49 mol), and [(mppyBr)$_2$Ir(hmacac)] (0.01 mol). Yield: 50%. ^{1}H NMR (400 MHz, $CDCl_3$): $\delta = 8.50$ (2H), 7.83–7.85 (4H), 7.77–7.73 (4H), 7.53–7.51 (2H), 4.40 (2H), 2.14 (4H), 1.95 (2H), 1.31–1.52 (7H), 1.1 (24H), 0.91–0.75 ppm (17H); ^{13}C NMR (100 MHz, $CDCl_3$): $\delta = 151.71$, 140.86, 140.43, 139.58, 133.12, 126.17, 125.54, 123.66, 121.70, 119.88, 118.97, 109.06, 108.92, 77.32, 77.01, 76.70, 55.38, 55.19, 43.38, 40.66, 31.81, 31.65, 30.13, 29.25, 29.08, 27.04, 23.92, 22.60, 14.03 ppm; elemental analysis (%) calcd: C 87.91, H 9.19, N 2.21; found: C 87.36, H 9.60, N 2.06.

PFCzMppyIrhm4 (15): Monomer feed: **8** (0.5 mol), **9** (0.46 mol), and [(mppyBr)$_2$Ir(hmacac)] (0.04 mol). Yield: 49%. ^{1}H NMR (400 MHz, $CDCl_3$): $\delta = 8.50$ (2H), 7.86 (4H), 7.74 (4H), 7.52 (2H), 6.67, 6.40, 4.39 (2H), 2.12 (4H), 1.96 (2H), 1.51–1.34 (8H), 1.16 (24H), 0.91–0.75 ppm (15H); ^{13}C NMR (100 MHz, $CDCl_3$): $\delta = 151.71$, 140.86, 140.42, 139.57, 133.11, 126.18, 123.65, 121.70, 119.90, 118.97, 109.06, 77.33, 77.01, 76.69, 55.36, 43.43, 40.64, 31.81, 31.65, 30.12, 29.25, 29.08, 28.43, 27.04, 23.92, 22.60, 14.03 ppm; elemental analysis (%) calcd: C 86.10, H 8.97, N 2.24; found: C 85.39, H 9.28, N 1.94.

PFCzMppyIrhm10 (16): Monomer feed: **8** (0.5 mol), **9** (0.4 mol), and [(mppyBr)$_2$Ir(hmacac)] (0.1 mol) Yield: 47%. H NMR (400 MHz, $CDCl_3$): $\delta = 8.52$ (2H), 7.87–7.73(10H), 7.65–7.55(3H), 7.49, 6.70, 6.41, 4.40 (2H), 2.14 (6H), 1.97 (2H), 1.48–1.27 (8H), 1.20 (29H), 0.91–0.77 ppm (18H); ^{13}C NMR (100 MHz, $CDCl_3$): $\delta = 151.74$, 140.89, 140.45, 139.60, 133.14, 128.78, 127.22, 126.20, 125.56, 123.68, 121.71, 119.91, 118.98, 109.08, 77.34, 77.02, 76.70, 55.39, 43.44, 40.66, 31.83, 31.67, 30.14, 29.27, 29.10, 28.45, 27.05, 23.94, 22.61, 14.04 ppm; elemental analysis (%) calcd: C 82.92, H 8.58, N 2.30; found: C 84.03, H 8.45, N 3.21.

PFCzMppyIrhm20 (17): Monomer feed: **8** (0.5 mol), **9** (0.3 mol), and [(mppyBr)$_2$Ir(hmacac)] (0.2 mol). Yield**:** 45%. ^{1}H NMR (400 MHz, $CDCl_3$): $\delta = 8.48$ (2H), 8.03 (2H), 7.87–7.31 (30H), 7.24 (4H), 6.68(2H), 6.37 (2H), 5.72 (1H), 4.39 (3H), 2.10–1.97 (10H), 1.51–1.31 (12H), 1.25 (32H), 0.91–0.77 ppm (28H); ^{13}C NMR (100 MHz, $CDCl_3$): $\delta = 167.23$, 152.10, 151.73, 146.28, 142.16, 140.44, 139.60, 134.96, 128.76, 127.21, 126.08, 125.63, 123.62, 123.33, 122.89, 121.64, 120.71, 120.24, 119.90, 119.59, 118.97, 117.32, 109.07, 89.46, 77.32, 77.00, 76.68, 55.51, 55.35, 43.40, 41.37, 40.50, 31.75, 31.56, 30.07, 29.23, 28.94, 28.42, 27.43, 27.03, 26.95, 23.91, 22.57, 21.73, 14.02 ppm; elemental analysis (%) calcd: C 78.56, H 8.06, N 2.39; found: C 75.95, H 7.33, N 2.61.

Fluorene-*alt*-carbazole (PFCz, 18): Monomer feed: **8** (0.5 mol) and **9** (0.5 mol). ^{1}H NMR (400 MHz, $CDCl_3$): $\delta = 8.52$ (2H), 7.5–7.84 (10H), 4.38 (2H), 2.03–2.13 (4H), 1.95 (2H), 1.11–1.52 (9H), 1.1 (24H), 0.74–0.89 ppm (16H); ^{13}C NMR (100 MHz, $CDCl_3$): $\delta = 151.69$, 140.84, 139.55, 133.10, 126.15, 123.63, 121.67, 119.87, 118.93, 109.04, 77.30, 76.99, 76.67, 56.95, 55.35, 40.63, 31.79, 30.10, 29.23, 29.06, 27.02, 23.90, 22.57, 14.01 ppm; elemental analysis (%) calcd for $(C_{29}H_{40})_{50}(C_{18}H_{19}N)_{50}$: C 88.48, H 9.32, N 2.20; found: C 88.03, H 9.33, N 1.88.

LED fabrication and characterization Polymers were dissolved in *p*-xylene and filtered through a filter (0.45 μm). Patterned glass substrates coated with indium tin oxide (ITO) were cleaned with acetone, detergent, distilled water, and 2-propanol, and subsequently in an ultrasonic bath. After treatment with oxygen plasma, poly-(3,4-ethylenedioxythiophene) (PEDOT) doped with poly(styrenesulfonic acid) (PSS; Batron-P 4083, Bayer AG) (150 nm) was spin-coated onto the ITO substrate followed by drying in a vacuum oven at 80 °C for 8 h. A thin film of polymers was coated onto the anode by spin casting in a dry box. The film thickness of the active layers was around 75–80 nm, measured with an Alfa Step 500 surface profiler (Tencor). A thin layer of Ba (4–5 nm) and a layer of Al (200 nm) were vacuum-evaporated subsequently on the top of the EL polymer layer under a vacuum of 1×10^{-4} Pa. Device performance was measured in a dry box. Current–voltage (*J*–*V*) characteristics were recorded with a Keithley 236 source meter. EL spectra were recorded by an Oriel Instaspec IV CCD Spectrograph. Luminance was measured by a PR 705 photometer (Photo Research). The external quantum efficiencies were determined by a Si photodiode with calibration in an integrating sphere (IS080, Labsphere).

Acknowledgements

The authors are grateful to the Ministry of Science and Technology of China (No. 2002CB613403), the National Natural Science Foundation of China (No. 50173008,) and the Natural Science Foundation of Guangdong Province (No. 11545) for their financial support of our work.

[1] a) Y. G. Ma, H. Y. Zhang, J. C. Shen, C. M. Chen, *Synth. Met.* **1998**, *94*, 245–248; b) M. A. Baldo, D. F. O'Brien, Y. You, A. Shoustikov, S. Sibley, M. E. Thompson, S. R. Forrest, *Nature* **1998**, *395*, 151; c) D. F. O'Brien, M. A. Baldo, M. E. Thompson, S. R. Forrest, *Appl. Phys. Lett.* **1999**, *74*, 442–444; d) C. Adachi, M. A. Baldo, S. R. Forrest, M. E. Thompson, *Appl. Phys. Lett.* **2000**, *77*, 904–906; e) Y. Wang, N. Herron, V. V. Grushin, D. Lecloux, V. Petrov, *Appl. Phys. Lett.* **2001**, *79*, 449–451; f) X. Z. Jiang, A. K.-Y. Jen, B. Carlson, L. R. Dalton, *Appl. Phys. Lett.* **2002**, *80*, 713–715; g) E. Stathatos, P. Lianos, E. Evgeniou, A. D. Keramidas, *Synth. Met.* **2003**, *139*, 2, 433-437.

[2] S. Lamansky, P. Djurovich, D. Murphy, F. Abdel-Razaq, H.-E. Lee, C. Adachi, P. E. Burrows, S. R. Forrest, M. E. Thompson, *J. Am. Chem. Soc.* **2001**, *23*, 4304–4312.

[3] C. Adachi, M. A. Baldo, M. E. Thompson, S. R. Forrest, *J. Appl. Phys.* **2001**, *90*, 5048–5051.

[4] a) D. F. O'Brien, C. Giebeler, R. B. Fletcher, A. J. Cadby, L. C. Palilis, D. G. Lidzey, P. A. Lane, D. D. C. Bradley, W. Blau, *Synth. Met.* **2001**, *116*, 379–383; b) P. A. Lane, L. C. Palilis, D. F. O'Brien, C. Giebeler, A. J. Cadby, D. G. Lidzey, A. J. Campbell, W. Blau, D. D. C. Bradley, *Phys. Rev. B* **2001**, *63*, 23, 5206; c) X. Gong, M. R. Robinson, J. C. Ostrowski, D. Moses, G. C. Bazan, A. J. Heeger, *Adv. Mater.* **2002**, *14*, 581–585.

[5] C. Y. Jiang, W. Yang, J. B. Peng, S. Xiao, Y. Cao, *Adv. Mater.* **2004**, *16*, 537–541.

[6] C. L. Lee, N. G. Kang, Y. S. Cho, J. S. Lee, J. J. Kim, *Opt. Mater.* **2003**, *21*, 119–123.

[7] S. Tokito, M. Suzuki, F. Sato, M. Kamachi, K. Shirane, *Org. Electron.* **2003**, *4*, 105–111.

[8] X. Chen, J.-L. Liao, Y. Liang, M. O. Ahmed, H.-E. Tseng, S.-A. Chen, *J. Am. Chem. Soc.* **2003**, *125(3)*, 636–637.

[9] A. J. Sandee, C. K. Williams, N. R. Evans, J. E. Davies, C. E. Boothby, A. Köhler, R. H. Friend, A. B. Holmes, *J. Am. Chem. Soc.* **2004**, *126*, 7041–7048.

[10] a) Q. Hou, Y. Xu, W. Yang, M. Yuan, J. Peng, Y. Cao, *J. Mater. Chem.* **2002**, *12*, 2887–2892; b) R. Q. Yang, R. Y. Tian, Q. Hou, W. Yang, Y. Cao, *Macromolecules* **2003**, *36*, 7453–7460.

[11] a) P. Nguyen, P. Gomez-Elipe, I. Manners, *Chem. Rev.* **1999**, *99*, 1515–1548; b) R. P. Kingsborough, T. M. Swage, *Prog. Inorg. Chem.* **1999**, *48*, 123- 231.

[12] B. Wang, M. R. Wasielewski, *J. Am. Chem. Soc.* **1997**, *119*, 12–21.

[13] U. S. Schubert, C. Eschbaumer, *Angew. Chem.* **2002**, *114*, 3016–3050; *Angew. Chem. Int. Ed.* **2002**, *41*, 2892–2926.

[14] M. Rehahn, *Acta Polymer.* **1998**, *49*, 201- 224.

[15] a) W.-Y. Wong, G.-L. Lu, K.-H. Choi, J.-X. Shi, *Macromolecules* **2002**, *35*, 3506–3513; b) M. S. Khan, M. R. A. Al-Mandhary, M. K. Al-Suti, A. K. Hisahm, P. R. Raithby, B. Ahrens, M. F. Mahon, L. Male, E. A. Marseglia, E. Tedesco, R. H. Friend, A. Köhler, N. Feeder, S. J. Teat, *J. Chem. Soc. Dalton Trans.* **2002**, 1358–1368.

[16] a) F. C. Chen, Y. Yang, M. E. Thompson, J. Kido, *Appl. Phys. Lett.* **2002**, *80*, 2308–2310; b) K. Brunner, A. Dijken, H. Börner, J. J. A. M. Bastiaansen, N. M. M. Kiggen, B. M. W. Langeveld, *J. Am. Chem. Soc.* **2004**, *126*, 6035–6042.

[17] W. T . Jefferson, Z. Sonja, *J. Org. Chem.* **1988**, *53*, 386–390.

[18] Y. Li, J. F. Ding, M. Day, Y. Tao, J. P. Lu, M. D'iorio, *Chem. Mater.* **2004**, *16*, 2165–2173.

[19] a) M. G. Colombo, A. Hauser, H. U. Gudel, *Inorg. Chem.* **1993**, *32*, 3088–3092; b) B. Schimid, F. O. Garces, R. J. Watts, *Inorg. Chem.* **1994**, *33*, 9–14.

[20] J. L. Bredas, R. Silbey, D. S. Boudreaux, R. R. Chance, *J. Am. Chem. Soc.* **1983**, *105*, 6555–6559.

[21] K. Brunner, A. Dijken, H. Borner, J. J. A. M. Bastiaansenl, N. M. M. Kiggen, B. M. W. Langeveld, *J. Am. Chem. Soc.* **2004**, *126*, 7718–7727.

[22] X. Gong, J. C. Ostrowski, D. Moses, G. C. Bazan, A. J. Heeger, *Adv. Funct. Mater.* **2003**, *13*, 439–444.

[23] a) C. Adachi, M. A. Baldo, S. R. Forrest, S. Lamansky, M. E. Thompson, R. C. Kwong, *Appl. Phys. Lett.* **2001**, *78*, 1622–1624; b) W. G. Zhu, Y. Q. Mo, L. J. Su, W. Yang, Y. Cao, *Appl. Phys. Lett.* **2002**, *80(12)*, 2045–2047.

[24] a) P. A. Lane, L. C. Palilis, D. F. O'Brien, C. A. Giebeler, J. Cadby, D. G. Lidzey, A. J. Campbell, W. Blau, D. D. C. Bradley, *Phys. Rev. B* **2001**, *63*, 5206; b) N. Tessler, P. K. H. V. Cleave, D. J. Pinner, R. H. Friend, G. Yahioglu, P. Le. Barny, J. Gray, M. D. Souza, G. Rumbles, *Thin Solid Films* **2000**, *363*, 64–67.

[25] X. Gong, J. C. Ostrowski, G. C. Bazan, D. Moses, A. J. Heeger, M. S. Liu, A. K. Y. Jen, *Adv. Mater.* **2003**, *15*, 45–49.

[26] Z. Wang, A. R. McWilliams, C. E. B. Evans, X. Lu, S. Chung, M. A. Winnik, I. Manners, *Adv. Funct. Mater.* **2002**, *12*, 415–419.

[27] S. Lamansky, P. Djurovich, D. Murphy, F. Abdel-Razzaq, R. Kwong, I. Tsyba, M. Bortz, B. Mui, R. Bau, M. E. Thompson, *Inorg. Chem.* **2001**, *40*, 1704–1711.

[28] a) J. K. Lee, G. Klaerner, R. D. Miller, *Chem. Mater.* **1997**, *9*, 1083–1088.

[29] a) M. Ranger, D. Rondeau, M. Leclerc, *Macromolecules* **1997**, *30*, 7686–7691; b) W. Yang, Q. Hou, C. Z. Liu, Y. H. Niu, J. Huang, R. Q. Yang, Y. Cao, *J. Mater. Chem.* **2003**, *13*, 1351–1355.

[30] J. Huang, Y. H. Niu, W. Yang, Y. Q. Mo, M. Yuan, Y. Cao, *Macromolecules* **2002**, *35*, 6080–6082.

[31] a) I. D. Rees, K. L. Robinson, A. B. Holmes, C. R. Towns, R. O'Dell, *MRS Bull.* **2002**, *27*, 451–455; b) I. Allen, T. Pounds, L. Murtagh, P. Wallace, C. Towns, WO 035796 A1, **2003**.

Received: November 28, 2004
Revised: April 16, 2005
Published online: June 23, 2005